

# Analytic Models for the Capacity Distribution in MDG-impaired Optical SDM Transmission

Lucas Zischler, *Student Member, OSA*, and Darli A. A. Mello, *Member, IEEE*

**Abstract**—In coupled space-division multiplexing (SDM) transmission systems, imperfections in optical amplifiers and passive devices introduce mode-dependent loss (MDL) and gain (MDG). These effects render the channel capacity stochastic and result in a decrease in average capacity. Several previous studies employ multi-section simulations to model the capacity of these systems. Additionally, relevant works derive analytically the capacity distribution for a single-mode system with polarization-dependent gain and loss (mode count  $D = 2$ ). However, to the best of our knowledge, analytic expressions of the capacity distribution for systems with  $D > 2$  have not been presented. In this paper, we provide analytic expressions for the capacity of optical systems with arbitrary mode counts. The expressions rely on Gaussian approximations for the per-mode capacity distributions and for the overall capacity distribution, as well as on fitting parameters for the capacity cross-correlation among different modes. Compared to simulations, the derived analytical expressions exhibit a suitable level of accuracy across a wide range of practical scenarios.

**Index Terms**—Space division multiplexing, channel capacity, channel models, optical fiber communications.

## I. INTRODUCTION

THE INCREASED capacity of multi-mode or multi-core fibers is a field of active research to handle the growing data traffic [1]–[6]. However, unequal gains in amplifiers or unequal losses in passive devices and fibers generate an effect known as mode-dependent gain (MDG) and mode-dependent loss (MDL). In systems with MDG or MDL, the spatial coupling during fiber propagation turns the channel capacity into a random variable, introducing a probability of outage [7]. Communications systems with a stochastic signal-to-noise ratio (SNR) need to be designed to maintain the outage probability below accepted levels. To properly assess outages in the design of future space-division multiplexing (SDM) systems, statistical models for the capacity are necessary.

The capacity loss statistics for a set of amplification schemes are discussed in [8]. Expressions for the variance of the per-mode capacity loss for four different amplification schemes are derived. However, both per-mode capacity and total capacity distributions are not analysed. [9]. Distributions for the per-mode modal gains have been presented in [10]. In addition, the paper obtains a closed-form expression for the average capacity. However, the capacity variance is not calculated. The impact of frequency diversity on the capacity distribution has

been discussed in [11], but no analytical expression for the capacity distribution has been presented. The exact distribution for a single-mode-fiber optical system with polarization-dependent gain (PDG,  $D = 2$ ) has been presented in [9]. However, the statistics of SDM systems with higher mode counts have been addressed by simulation.

In this paper, we provide analytical expressions for the variance of the capacity distribution<sup>1</sup>. The derivations are based on the assumption of a Gaussian distribution for the per-mode marginal capacity probability density function (PDF). The joint capacity distribution is approximated as a multivariate normal, and the total capacity is obtained as the linear combination of the marginals [12]. The derivations rely on the modal gain distributions outlined in [10].

## II. INSTANTANEOUS CAPACITY

Assuming no channel state information (CSI), the instantaneous capacity of a narrowband SDM channel is given by [13]

$$C_T = \log_2 \left( \det [\mathbf{I} + \text{SNR} \cdot \mathbf{H}\mathbf{H}^H] \right), \quad (1)$$

where SNR is the ratio of total signal power and total noise power,  $\mathbf{H}$  is the channel transfer matrix, and  $\mathbf{I}$  is the identity matrix of size  $D$ , where  $D$  is the mode count.

The total capacity can be obtained from the eigenvalues  $\lambda$  of the  $\mathbf{H}\mathbf{H}^H$  [13] operator

$$C_T = \sum_{i=1}^D C_i = \sum_{i=1}^D \log_2 (1 + \text{SNR} \cdot \lambda_i), \quad (2)$$

where  $\lambda_i$  is the  $i^{\text{th}}$  mode gain experienced in the system. Considering the noise as spatially white, the noise power is distributed equally between the modes, and the total signal power must be distributed such that the sum of all mode powers is constant in respect to MDG, and the average power ratio between total and individual signal power is  $1:1/D$ . The sum of all  $\lambda$  should then be equal to  $D$ , with an expected gain per mode  $\mathbb{E}\{\lambda\} = 1$  over all  $D$  modes.

Equation (2) provides the capacity for a single channel realization. As in MDG-impaired systems the capacity is a random variable, the distribution of  $\lambda_i$  must also be taken into account. Reference [10] demonstrates that the overall PDF of the  $\lambda$  eigenvalues, in decibels, can be given by the well-known Gaussian unitary ensemble (GUE) spectral distribution. The model is derived from random matrix theory, where a statistical behavior is observed for unspecified eigenvalues [14], [15]. However, obtaining closed-form analytical

<sup>1</sup>An analytical solution for the total capacity mean is presented [10, Eq. (10)].

Manuscript received XXX xx, XXXX; revised XXXXX xx, XXXX; accepted XXXX XX, XXXX. This work was financed in part by the Coordenação de Aperfeiçoamento de Pessoal de Nível Superior – Brasil (CAPES) – Finance Code 001.

L. Zischler, and D. A. A. Mello are with the School of Electrical and Computer Engineering, State University of Campinas, Campinas 13083-970, Brazil: (e-mail: l257176@dac.unicamp.br).

models for the individual marginal eigenvalue distributions is not trivial, except for specific cases, such as low eigenvalue counts ( $D \leq 3$ ) [16], or for the smallest and largest eigenvalues as specified by the Tracy-Widom distribution [17].

### III. MARGINAL CAPACITY DISTRIBUTIONS

We evaluate the statistics of the total capacity  $C_T$  based on the per-mode marginal  $\lambda_i$  and  $C_i$  distributions. Approximations on  $C_i$  distributions are obtained from two methods derived from the GUE spectral and Wigner semicircular distribution marginals for  $\lambda_i$ .

#### A. Approximations on the $C_i$ distribution based on the GUE spectral distribution for $\lambda_i$

The total distribution of the  $\lambda_{\text{dB}}$  eigenvalues for a  $D^{\text{th}}$  order GUE is given by [10]

$$f_{\lambda_{\text{dB}}}(\lambda_{\text{dB}}) = \frac{\alpha_{\lambda_{\text{dB}},D}}{\sigma_{\text{mdg}}} e^{-\frac{(D+1)}{2} \left( \frac{\lambda_{\text{dB}} - \mu_{\lambda_{\text{dB}}}}{\sigma_{\text{mdg}}} \right)^2} \sum_{k=0}^{D-1} \beta_{\lambda_{\text{dB}},D,k} \left( \frac{\lambda_{\text{dB}} - \mu_{\lambda_{\text{dB}}}}{\sigma_{\text{mdg}}} \right)^{2k} \quad (3)$$

where  $\alpha_{\lambda_{\text{dB}},D}$  is a normalization factor such that the PDF integral equals 1, and  $\beta_{\lambda_{\text{dB}},D,k}$  are the polynomial coefficients.  $\alpha_{\lambda_{\text{dB}},D}$  and  $\beta_{\lambda_{\text{dB}},D,k}$  are constant for a given number of modes. For  $D \leq 8$  the values of  $\alpha_{\lambda_{\text{dB}},D}$  and  $\beta_{\lambda_{\text{dB}},D,k}$  are provided in [10, Table 1], and the derivation of the coefficients is presented in further detail in [16]. Values<sup>2</sup>  $\sigma_{\text{mdg}}$  and  $\mu_{\lambda_{\text{dB}}}$  are the standard deviation and the mean of  $f_{\lambda_{\text{dB}}}(\lambda_{\text{dB}})$ , respectively. Value  $\mu_{\lambda_{\text{dB}}}$  is given such that the linearised eigenvalue distribution  $f_{\lambda}(\lambda)$  has unitary mean, and is given by (see appendix A)

$$\mu_{\lambda_{\text{dB}}} = -10 \cdot \log_{10} \left[ \int_{-\infty}^{\infty} 10^{\frac{x}{10}} \widehat{f}_{\lambda_{\text{dB}}}(x) dx \right], \quad (4)$$

where  $\widehat{f}_{\lambda_{\text{dB}}}(x)$  is the zero mean  $\lambda_{\text{dB}}$  distribution.

We assume that the means of  $f_{\lambda_{\text{dB},i}}(\lambda_{\text{dB},i})$ , given  $i \in [1, D]$ , are near the local maxima of the  $f_{\lambda_{\text{dB}}}(\lambda_{\text{dB}})$  PDF. We further assume that the marginal distributions can be represented by Gaussian distributions, with standard deviation  $\sigma_{\lambda_{\text{dB},i}}$  and mean  $\mu_{\lambda_{\text{dB},i}}$ . The ordering of the indices is given by their mean value, such that  $\mu_{\lambda_{\text{dB},1}} \leq \mu_{\lambda_{\text{dB},2}} \leq \dots \leq \mu_{\lambda_{\text{dB},D}}$ .

The approximated  $\mu_{\lambda_{\text{dB},i}}$  values are obtained from the odd index zeros of the overall PDF derivative, detailed in appendix B, given in a simplified form as

$$\sum_{k=0}^{D-1} \frac{\beta_{\lambda_{\text{dB}},D,k}}{\sigma_{\text{mdg}}^{2k}} \left[ 2k \cdot (\mu_{\lambda_{\text{dB},i}} - \mu_{\lambda_{\text{dB}}})^{2k-1} - \frac{D+1}{\sigma_{\text{mdg}}^2} (\mu_{\lambda_{\text{dB},i}} - \mu_{\lambda_{\text{dB}}})^{2k+1} \right] = 0. \quad (5)$$

<sup>2</sup>The notation  $\sigma_{\text{mdg}}$  was preferred to  $\sigma_{\lambda_{\text{dB}}}$ , as the former is predominant in literature.

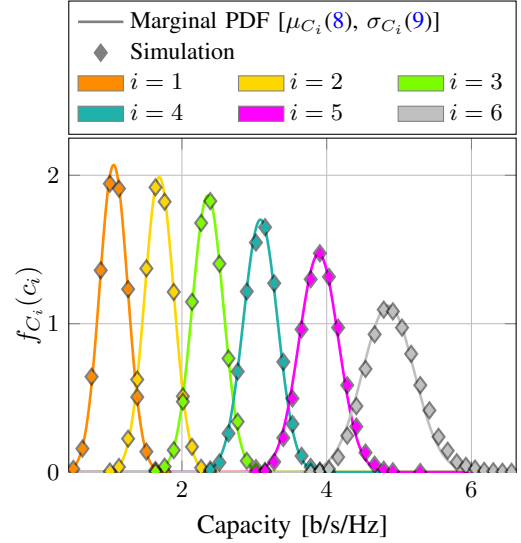


Fig. 1: Gaussian marginal PDFs for  $D = 6$ , SNR = 10 dB, and  $\sigma_{\text{mdg}} = 5$  dB.

The values of  $\sigma_{\lambda_{\text{dB},i}}$  are obtained such that the overall and marginal PDF values at  $\mu_{\lambda_{\text{dB},i}}$  are equal, given a normalization factor of  $1/D$

$$\sigma_{\lambda_{\text{dB},i}} = \frac{1}{D\sqrt{2\pi}f_{\lambda_{\text{dB}}}(\mu_{\lambda_{\text{dB},i}})}. \quad (6)$$

From the obtained  $\mu_{\lambda_{\text{dB},i}}$  and  $\sigma_{\lambda_{\text{dB},i}}$ , the marginal PDF can be approximated as a Gaussian distribution

$$f_{\lambda_{\text{dB},i}}(\lambda_{\text{dB},i}) = \frac{1}{\sigma_{\lambda_{\text{dB},i}}\sqrt{2\pi}} e^{-\frac{1}{2} \left( \frac{\lambda_{\text{dB},i} - \mu_{\lambda_{\text{dB},i}}}{\sigma_{\lambda_{\text{dB},i}}} \right)^2}. \quad (7)$$

The relation between the marginal distribution of eigenvalues  $f_{\lambda_{\text{dB}}}(\lambda_{\text{dB}})$  and the marginal distribution of capacities  $f_{C_i}(c_i)$  is obtained by transformation as

$$f_{C_i}(c_i) = \frac{10 \cdot \ln(2) 2^{c_i}}{\ln(10) (2^{c_i} - 1)} f_{\lambda_{\text{dB},i}} \left( \frac{10}{\ln(10)} \ln \left( \frac{2^{c_i} - 1}{\text{SNR}} \right) \right). \quad (8)$$

Applying the same proposition as for  $\lambda_{\text{dB},i}$ , the distribution of  $C_i$  can be also approximated as a Gaussian distribution with standard deviation  $\sigma_{C_i}$  and mean  $\mu_{C_i}$ . Setting the derivative of (8) to zero (see appendix C), the value of  $\mu_{C_i}$  can be obtained as the solution of the simplified equation

$$\frac{10 \cdot 2^{\mu_{C_i}}}{\sigma_{\lambda_{\text{dB},i}}^2 \ln(10)} \left( \frac{10}{\ln(10)} \ln \left( \frac{2^{\mu_{C_i}} - 1}{\text{SNR}} \right) - \mu_{\lambda_{\text{dB},i}} \right) + 1 = 0. \quad (9)$$

The values of  $\sigma_{C_i}$  are that obtained by setting the Gaussian approximation and (8) equal at  $\mu_{C_i}$ , which is achieved for

$$\sigma_{C_i} = \frac{1}{\sqrt{2\pi}f_{C_i}(\mu_{C_i})}. \quad (10)$$

The result of the Gaussian approximation for  $f_{C_i}$ , for a system with  $D = 6$ , SNR = 10 dB and  $\sigma_{\text{mdg}} = 5$  dB, is shown in Fig. 1. The results reveal an excellent agreement between the simulation and the derived analytical curves. A statistical analysis for  $2 \leq D \leq 8$  is presented in Fig. 2, showing again an excellent agreement.

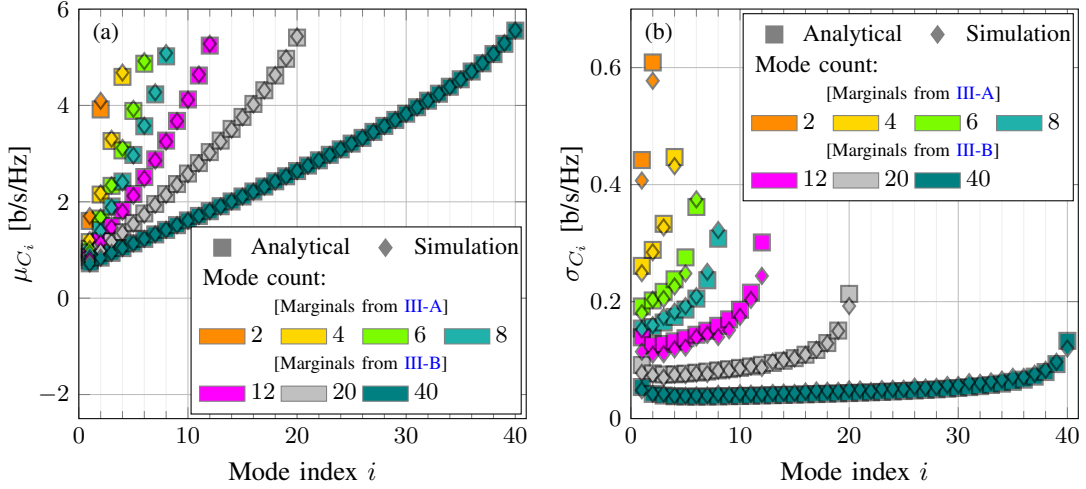


Fig. 2: Analytical approximation of marginal capacity PDFs for SNR = 10 dB and  $\sigma_{mdg} = 5$  dB. For  $D \leq 8$  the GUE distribution method is considered, for higher mode counts, the Wigner semicircular cumulative distribution function (CDF) method is utilized.

### B. Approximations on the $C_i$ distribution based on the Wigner semicircular distribution for $\lambda_i$

The limit distribution of  $\lambda_{dB}$  as  $D \rightarrow \infty$  is given by the Wigner semicircular distribution as [10], [14]

$$f_{\lambda_{dB}}(\lambda_{dB}) = \frac{1}{2\pi\sigma_{mdg}} \sqrt{4 - \frac{(\lambda_{dB} - \mu_{\lambda_{dB}})^2}{\sigma_{mdg}^2}}, \quad (11)$$

$$-2\sigma_{mdg} + \mu_{\lambda_{dB}} \leq \lambda_{dB} \leq 2\sigma_{mdg} + \mu_{\lambda_{dB}},$$

with  $\mu_{\lambda_{dB}}$  given in (4).

For this limiting case, the capacity PDF and CDF for an unspecified mode are analytically obtainable. The capacity PDF is obtained applying (11) in (8) and is given by

$$f_C(c) = \frac{5 \cdot \ln(2) 2^c}{\pi \sigma_{mdg} \ln(10) (2^c - 1)} \sqrt{4 - \frac{1}{\sigma_{mdg}^2} \left( \frac{10}{\ln(10)} \ln \left( \frac{2^c - 1}{\text{SNR}} \right) - \mu_{\lambda_{dB}} \right)^2}, \quad (12)$$

and the CDF, developed in further detail in appendix D, is given by

$$F_C(c) = \frac{1}{2} + \left( \frac{5}{\pi \sigma_{mdg} \ln(10)} \ln \left( \frac{2^c - 1}{\text{SNR}} \right) - \frac{\mu_{\lambda_{dB}}}{2\pi \sigma_{mdg}} \right) \sqrt{1 - \left( \frac{5}{\sigma_{mdg} \ln(10)} \ln \left( \frac{2^c - 1}{\text{SNR}} \right) - \frac{\mu_{\lambda_{dB}}}{2\sigma_{mdg}} \right)^2} + \frac{1}{\pi} \sin^{-1} \left( \frac{5}{\sigma_{mdg} \ln(10)} \ln \left( \frac{2^c - 1}{\text{SNR}} \right) - \frac{\mu_{\lambda_{dB}}}{2\sigma_{mdg}} \right), \quad (13)$$

where both distributions have the following limits

$$\log_2 \left( \text{SNR} \cdot 10^{\frac{\mu_{\lambda_{dB}} - 2\sigma_{mdg}}{10}} + 1 \right) \leq c \leq \log_2 \left( \text{SNR} \cdot 10^{\frac{\mu_{\lambda_{dB}} + 2\sigma_{mdg}}{10}} + 1 \right). \quad (14)$$

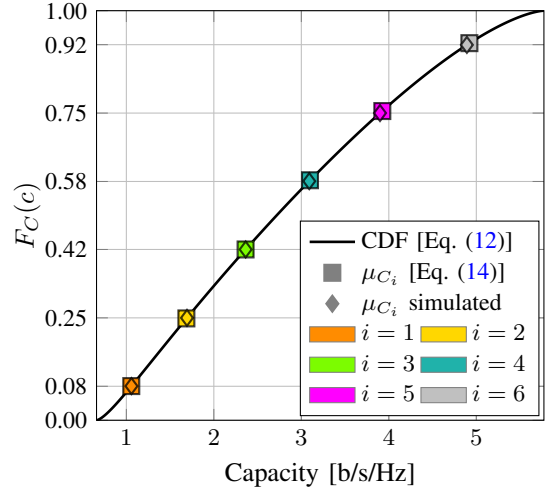


Fig. 3: Capacity CDF and  $\mu_{C_i}$  estimation for  $D = 6$ , SNR = 10 dB, and  $\sigma_{mdg} = 5$  dB.

From the assumption that the marginal PDFs are symmetric and with minimal overlap, the values of  $\mu_{C_i}$  can be obtained from the CDF as the solutions to

$$\frac{i - 1/2}{D} = F_C(\mu_{C_i}). \quad (15)$$

An assessment of this approximation can be found in Fig. 3, for a system with  $D = 6$ , SNR = 10 dB and  $\sigma_{mdg} = 5$  dB, showing excellent agreement.

The values of  $\sigma_{C_i}$  can then be obtained from the total PDF and  $\mu_{C_i}$ , such as in (6), yielding

$$\sigma_{C_i} = \frac{1}{D\sqrt{2\pi}f_C(\mu_{C_i})}. \quad (16)$$

Differences between the predictions generated by the Wigner semicircular distribution and the GUE spectral are expected. The Wigner semicircular distribution flattens the

local maximums of the GUE spectral distribution, which are of important value for this methodology. However, the divergences fade as the mode count increases. In Fig. 2, the predictions for  $D = 12$ ,  $D = 20$  and  $D = 40$  were obtained based on the Wigner semicircle distribution. A noticeable  $\sigma_{C_i}$  error is perceived at  $D = 12$ , due to the Wigner semicircular divergence from the real distribution. This error is less significant as the mode count increases.

#### IV. TOTAL CAPACITY DISTRIBUTION

Owing to correlations between  $\lambda_i$  variables, the marginal distributions are not sufficient to model the statistical parameters of the total capacity. As seen in Fig. 1, the distributions of marginal capacities closely approximate normal distributions. In this work, we propose that the joint PDF of the capacity can be approximated as a multivariate normal distribution. A sum of individual elements of a multivariate normal distribution has a normal distribution given by

$$f_{C_T}(c_T) = \frac{1}{\sigma_{C_T} \sqrt{2\pi}} e^{-\frac{1}{2} \left( \frac{c_T - \mu_{C_T}}{\sigma_{C_T}} \right)^2}, \quad (17)$$

where the generalized variance  $\sigma_{C_T}^2$  and total mean  $\mu_{C_T}$  can be obtained, respectively, by

$$\begin{aligned} \sigma_{C_T}^2 &= \sum_{i,j=1,1}^{D,D} \sigma_{C_i} \sigma_{C_j} \rho_{i,j} \\ \mu_{C_T} &= \sum_{i=1}^D \mu_{C_i}. \end{aligned} \quad (18)$$

Alternatively, an already proposed exact solution for  $\mu_{C_T}$  has been proposed in [9], [10]

$$\mu_{C_T} = D \int_{-\infty}^{\infty} \log_2 \left( 1 + \text{SNR} \cdot 10^{\frac{\sigma_{\text{mdg}} x + \mu_{\lambda_{\text{dB}}}}{10}} \right) \tilde{f}_{\lambda_{\text{dB}}}(x) dx, \quad (19)$$

where  $\tilde{f}_{\lambda_{\text{dB}}}(x)$  is the unitary variance, zero mean  $\lambda_{\text{dB}}$  distribution.

In (18),  $\rho_{i,j}$  is the correlation coefficient between the  $i^{\text{th}}$  and  $j^{\text{th}}$  capacity PDFs. The correlation coefficient is related to the covariance by

$$\rho_{i,j} = \frac{\text{cov}(C_i, C_j)}{\sigma_{C_i} \sigma_{C_j}}. \quad (20)$$

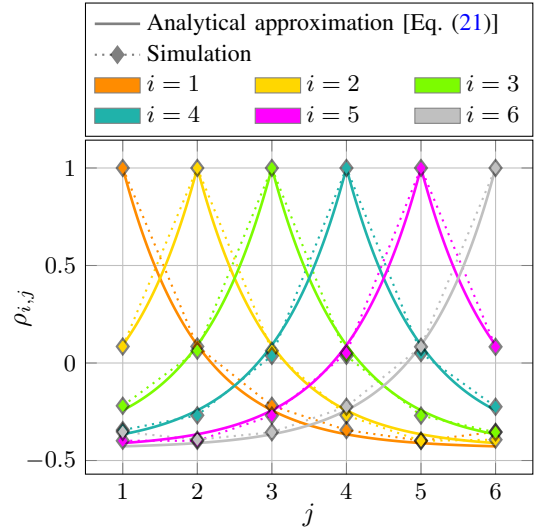


Fig. 4: Correlation for  $D = 6$ ,  $\text{SNR} = 10$  dB, and  $\sigma_{\text{mdg}} = 5$  dB.

An exact equation for  $\rho_{i,j}$  is unknown, however, as observed in Fig. 4, a suitable empirical approximation is given by

$$\rho_{i,j} = e^{-|i-j|} + \left( e^{-|i-j|} - 1 \right) (\gamma_0 + \gamma_1 \cdot \sigma_{\text{mdg}}^{2.75}), \quad (21)$$

where the coefficients  $\gamma_0$  and  $\gamma_1$  are unique to a given mode count and signal-to-noise ratio (SNR) value. In this paper, we numerically obtain the values of  $\gamma_0$  and  $\gamma_1$  such that the mean squared logarithmic error (MSLE) between analytical and simulation capacity variance is minimized, i.e.,

$$(\gamma_0, \gamma_1) = \underset{\gamma_0, \gamma_1}{\text{argmin}} \left( \mathbb{E} \left\{ \left[ \ln(\hat{\sigma}_{C_T}^2) - \ln(\sigma_{C_T}^2) \right]^2 \right\} \right). \quad (22)$$

The methodology to obtain the coefficients is performed iteratively until a tolerance threshold is reached. The algorithm implemented in this work firstly updates  $\gamma_0$  until the error for the lowest considered  $\sigma_{\text{mdg}}$  is smaller than a defined tolerance. The value of  $\gamma_1$  is updated considering the MSLE for the entire evaluated  $\sigma_{\text{mdg}}$  range, with small corrections to  $\gamma_0$  if the resulting approximation function is not monotonic increasing. We select the logarithmic error because the capacity variance scales exponentially in relation to  $\sigma_{\text{mdg}}$  when measured in

TABLE I: Correlation function coefficients.  $10^{-10}$  as  $\gamma_0$  error tolerance.  $10^4$  as  $\gamma_1$  iteration count tolerance.

	$D$	SNR = 5 dB		SNR = 10 dB		SNR = 15 dB		SNR = 20 dB	
		$\gamma_0$	$\gamma_1$	$\gamma_0$	$\gamma_1$	$\gamma_0$	$\gamma_1$	$\gamma_0$	$\gamma_1$
Method III-A	2	2.16297989	-1.424485E-3	2.16381222	-3.241463E-4	2.16393724	-5.664255E-5	2.16395171	-1.031541E-5
	3	1.09160893	6.095528E-4	1.09153003	1.498233E-4	1.09149336	4.022044E-5	1.09147997	7.691563E-6
	4	0.72791071	1.114647E-4	0.72795167	5.751291E-5	0.72793629	2.789583E-5	0.72792665	6.419168E-6
	5	0.54480425	-1.547994E-4	0.54492813	-2.174217E-5	0.54493125	1.038573E-5	0.54492585	5.543675E-6
	6	0.43511438	7.630925E-5	0.43513127	3.758373E-5	0.43512306	1.614824E-5	0.43511820	3.966745E-6
	7	0.36203898	-1.120187E-4	0.36211666	-1.754819E-5	0.36212190	4.308864E-6	0.36212014	3.102686E-6
	8	0.31008496	-1.768119E-4	0.31016253	-3.614410E-5	0.31017045	-2.168861E-6	0.31017007	1.195690E-6
	Method III-B	9	0.27114473	1.871205E-4	0.27107389	3.189872E-5	0.27106495	1.572890E-6	0.27106446
10		0.24115580	8.250165E-5	0.24113560	3.632280E-6	0.24113577	-4.177426E-6	0.24113686	-1.934882E-6
12		0.19777600	7.311636E-5	0.19775961	-1.298120E-7	0.19776223	-7.621126E-6	0.19776444	-3.509853E-6
20		0.11577972	-2.081275E-4	0.11585818	-7.543138E-5	0.11587780	-2.177745E-5	0.11588300	-6.367806E-6
30		0.07681464	-2.282790E-4	0.07689957	-8.327005E-5	0.07691975	-2.324244E-5	0.07692502	-6.536148E-6
40		0.05768991	-1.842371E-4	0.05776636	-6.941402E-5	0.05778465	-2.036533E-5	0.05778933	-5.994924E-6

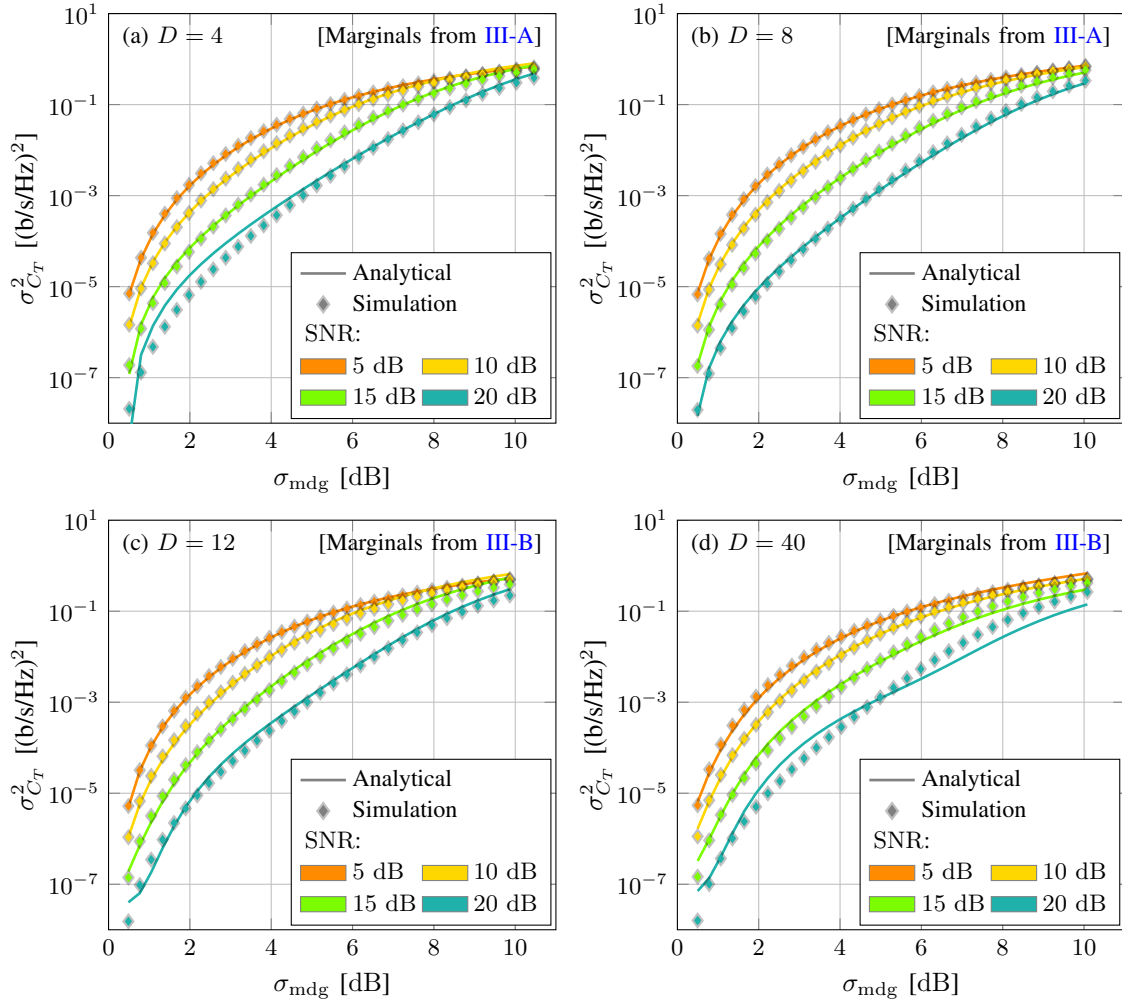


Fig. 5: Analytical estimation of the total capacity variance.

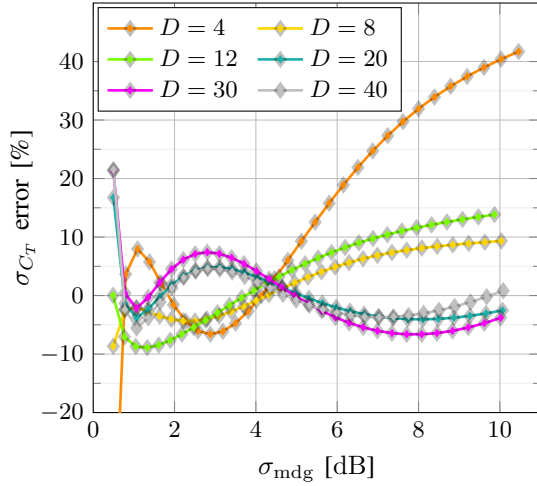


Fig. 6: Approximation error for SNR = 10 dB. For comparison fairness, all the marginal values are obtained from the Wigner semicircular CDF method.

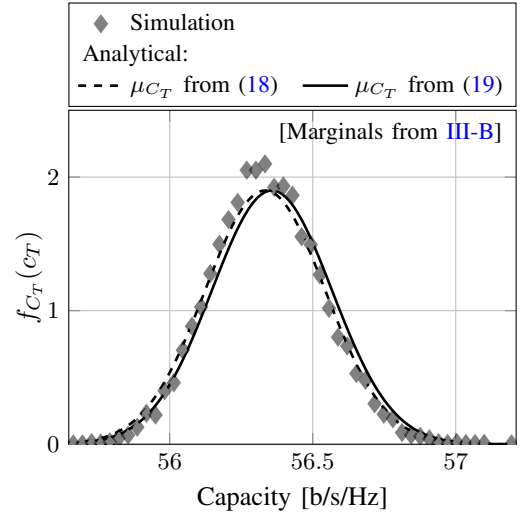


Fig. 7: Total Gaussian PDF for  $D = 20$ , SNR = 10 dB, and  $\sigma_{\text{mdg}} = 5$  dB.

decibels. The coefficients for a practical range of mode counts and SNR are given in table I.

An analysis comparing analytical and simulation values is presented in Fig. 5. The results indicate an accurate variance approximation for SNR values lower than 20 dB for all mode counts evaluated, with greater precision for high mode counts. For a SNR value of 20 dB, there is a high divergence for the estimation with the Wigner semicircular CDF method. The potential source of estimation discrepancies likely stems from the marginal distributions estimated from the capacity CDF, as well as approximations made in the correlation function. Fig. 6 evaluates the accuracy of the method based on Wigner semicircular CDF for different values of  $\sigma_{mdg}$  and mode counts. The results evidence accurate estimates for mode counts higher than 20. Fig. 7 compares the simulated total capacity distribution with the analytical distributions produced with the Wigner semicircular CDF method. The presented Gaussian approximation exhibit a good agreement with the simulated curve.

## V. IMPACT OF FREQUENCY DIVERSITY

In MDG-impaired systems, the random coupling among modes turns the capacity into a random variable, eventually generating outages. As demonstrated in [11], modal dispersion generates a frequency-dependent channel frequency response that mitigates the impact of deep fades. This effect, known as frequency diversity, has a beneficial impact on the outage capacity [18]. As seen in Fig. 8, the total capacity standard deviation has a weak dependence on the mode count, in agreement with [18]. This effect has been called mode diversity in [9]. According to the effect of mode diversity, the outage probability is more significant in lower mode counts, as fewer paths are available to mitigate outages.

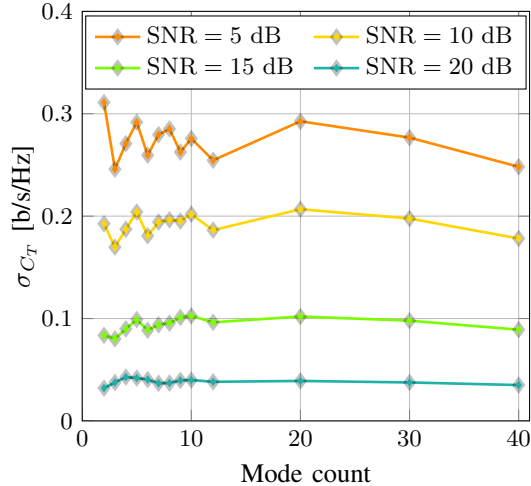


Fig. 8: Total capacity deviation per mode for  $\sigma_{mdg} = 5$  dB from the analytical equations.

So far, this paper considered a narrowband channel with a flat frequency response. However, as presented in [11], modal dispersion induces frequency-dependent mode gains. In this case, the total capacity in a given bandwidth can be calculated

by dividing the spectrum into  $N$  narrowband frequency bins and adding the corresponding capacities [9]. In this model, the channel response of a given frequency bin is independent of that in adjacent bins [11]. Considering the distributions presented in Section III, the averaged capacity variance of the  $i^{th}$  mode, considering  $N$  independent frequency bins is given by

$$\bar{\sigma}_{C_i}^2 = \frac{\sigma_{C_i}^2}{N}. \quad (23)$$

## VI. CONCLUSION

We propose statistical models that approximate the marginal per-mode and total capacity variances for strongly-coupled space division multiplexing (SDM) transmission systems. The model is based on the Gaussian assumption for the marginal per-mode capacity. The total capacity distribution is modeled as a joint multivariate normal distribution given by a linear combination of marginals. The marginal per-mode capacity distributions are derived by two methods, namely based on the GUE spectral distribution for the channel gains and on the Wigner semicircular distribution. The correlation between per-mode capacities is addressed by an empirical analytical model with fitting coefficients obtained by numerical simulations. The analytical results exhibit a suitable agreement with simulations in the investigated scenarios. The narrowband results can be extended to arbitrary bandwidths resorting to the existing theory on frequency diversity

## APPENDIX A

### EQUATION FOR $\mu_{\lambda_{dB}}$ FROM THE LINEARIZED EIGENVALUES MEAN

Given  $\lambda_{dB} = 10 \cdot \log_{10}(\lambda)$ , the linearized eigenvalue distribution is related to the  $\lambda_{dB}$  distribution by

$$f_{\lambda}(\lambda) = \frac{10}{\ln(10)\lambda} f_{\lambda_{dB}}(10 \cdot \log_{10}(\lambda)), \quad (24)$$

and the  $\lambda$  mean is given by

$$\mu_{\lambda} = \int_{-\infty}^{\infty} \frac{10}{\ln(10)} \hat{f}_{\lambda_{dB}}(10 \cdot \log_{10}(\lambda) - \mu_{\lambda_{dB}}) d\lambda, \quad (25)$$

where  $\hat{f}_{\lambda_{dB}}(\cdot)$  is the  $\lambda_{dB}$  distribution shifted by  $\mu_{\lambda_{dB}}$ , resulting in a zero mean PDF. Using  $x = 10 \cdot \log_{10}(\lambda) - \mu_{\lambda_{dB}}$  and  $dx = \ln(10) 10^{\frac{x+\mu_{\lambda_{dB}}}{10}}/10 d\lambda$ , after some manipulation we have

$$\mu_{\lambda_{dB}} = -10 \cdot \log_{10} \left[ \int_{-\infty}^{\infty} \frac{10^{\frac{x}{10}}}{\mu_{\lambda}} \hat{f}_{\lambda_{dB}}(x) dx \right]. \quad (26)$$

## APPENDIX B

### APPROXIMATION OF $\mu_{\lambda_{dB},i}$ FROM THE GUE DERIVATIVE

We propose that the marginal means  $\lambda_{dB}$  can be approximated by the  $f_{\lambda_{dB}}(\lambda_{dB})$  local maxima. Given that the GUE distribution is positive definite, the first  $\lambda_{dB}$  value for which  $f'_{\lambda_{dB}}(\lambda_{dB}) = 0$  is a local maximum, and the subsequent value is a local minimum. Maxima and minima alternate in a way such that odd solutions return local maxima. This can be demonstrated by guaranteeing that  $f''_{\lambda_{dB}}(\lambda_{dB}) < 0$  for the

$\lambda_{\text{dB}}$  values that fulfill  $f'_{\lambda_{\text{dB}}}(\lambda_{\text{dB}}) = 0$ . Expanding on the first derivative from (3), utilizing  $\widehat{\lambda}_{\text{dB}} = \lambda_{\text{dB}} - \mu_{\lambda_{\text{dB}}}$ , yields

$$\begin{aligned} f'_{\widehat{\lambda}_{\text{dB}}}(\widehat{\lambda}_{\text{dB}}) &= 0 \\ \frac{d}{d\widehat{\lambda}_{\text{dB}}} \left[ \frac{\alpha_{\lambda_{\text{dB}}, D}}{\sigma_{\text{mdg}}} e^{-\frac{(D+1)}{2} \frac{\widehat{\lambda}_{\text{dB}}^2}{\sigma_{\text{mdg}}^2}} \sum_{k=0}^{D-1} \beta_{\lambda_{\text{dB}}, D, k} \frac{\widehat{\lambda}_{\text{dB}}^{2k}}{\sigma_{\text{mdg}}^{2k}} \right] &= 0 \quad (27) \\ \frac{d}{d\widehat{\lambda}_{\text{dB}}} \left[ e^{-\frac{(D+1)}{2} \frac{\widehat{\lambda}_{\text{dB}}^2}{\sigma_{\text{mdg}}^2}} \sum_{k=0}^{D-1} \beta_{\lambda_{\text{dB}}, D, k} \frac{\widehat{\lambda}_{\text{dB}}^{2k}}{\sigma_{\text{mdg}}^{2k}} \right] &= 0. \end{aligned}$$

Setting  $g(\widehat{\lambda}_{\text{dB}}) = \sum_{k=0}^{D-1} \beta_{\lambda_{\text{dB}}, D, k} \frac{\widehat{\lambda}_{\text{dB}}^{2k}}{\sigma_{\text{mdg}}^{2k}}$  and  $\delta_0 = \frac{D+1}{2\sigma_{\text{mdg}}^2}$ ,

$$\begin{aligned} \frac{d}{d\widehat{\lambda}_{\text{dB}}} \left[ e^{-\delta_0 \widehat{\lambda}_{\text{dB}}^2} g(\widehat{\lambda}_{\text{dB}}) \right] &= 0 \\ g'(\widehat{\lambda}_{\text{dB}}) e^{-\delta_0 \widehat{\lambda}_{\text{dB}}^2} - 2\delta_0 \widehat{\lambda}_{\text{dB}} e^{-\delta_0 \widehat{\lambda}_{\text{dB}}^2} g(\widehat{\lambda}_{\text{dB}}) &= 0 \quad (28) \\ g'(\widehat{\lambda}_{\text{dB}}) - 2\delta_0 \widehat{\lambda}_{\text{dB}} g(\widehat{\lambda}_{\text{dB}}) &= 0, \end{aligned}$$

where  $g'(\widehat{\lambda}_{\text{dB}})$  is given by

$$g'(\widehat{\lambda}_{\text{dB}}) = \sum_{k=0}^{D-1} \frac{2k\beta_{\lambda_{\text{dB}}, D, k}}{\sigma_{\text{mdg}}^2} \widehat{\lambda}_{\text{dB}}^{2k-1}. \quad (29)$$

Applying (29) into (28), and replacing  $\widehat{\lambda}_{\text{dB}}$  by  $\mu_{\lambda_{\text{dB}, i}} - \mu_{\lambda_{\text{dB}}}$  yields (5) after some manipulation.

#### APPENDIX C

##### APPROXIMATION OF $\mu_{C_i}$ FROM MARGINAL CAPACITIES DERIVATIVE

From the same proposition that the marginal capacities PDF can be modeled as Gaussian, the means can be obtained from the solution to  $f'_{C_i}(c_i) = 0$ . The marginal capacity PDF is provided in (8). We also consider the following auxiliary elements

$$\begin{aligned} \delta_1 &= \frac{10 \cdot \ln(2)}{\sigma_{\lambda_{\text{dB}, i}} \ln(10) \sqrt{2\pi}}, \\ h_0(c_i) &= \frac{1}{\sigma_{\lambda_{\text{dB}, i}}} \left[ \frac{10}{\ln(10)} \ln \left( \frac{2^{c_i} - 1}{\text{SNR}} \right) - \mu_{\lambda_{\text{dB}, i}} \right], \quad (30) \\ h_1(c_i) &= e^{-\frac{h_0^2(c_i)}{2}}, \\ h_2(c_i) &= 2^{c_i} h_1(c_i). \end{aligned}$$

Applying (7) into (8), and applying the substitutions provided in (30), yields

$$f_{C_i}(c_i) = \frac{\delta_1}{(2^{c_i} - 1)} h_2(c_i), \quad (31)$$

with the derivative given by

$$f'_{C_i}(c_i) = \frac{\delta_1}{(2^{c_i} - 1)^2} [h'_2(c_i) (2^{c_i} - 1) - h_2(c_i) \ln(2) 2^{c_i}]. \quad (32)$$

The derivatives of the auxiliary functions in (30) are given by

$$\begin{aligned} h'_0(c_i) &= \frac{\delta_1 \sqrt{2\pi} \cdot 2^{c_i}}{(2^{c_i} - 1)} \\ h'_1(c_i) &= -h_0(c_i) h'_0(c_i) e^{-\frac{h_0^2(c_i)}{2}} \\ h'_2(c_i) &= 2^{c_i} (h'_1(c_i) + \ln(2) h_1(c_i)). \end{aligned} \quad (33)$$

Replacing these terms in (32) results in

$$\begin{aligned} f'_{C_i}(c_i) &= \frac{\delta_1 2^{c_i}}{(2^{c_i} - 1)^2} [(h'_1(c_i) + \ln(2) h_1(c_i)) (2^{c_i} - 1) \\ &\quad - 2^{c_i} \ln(2) h_1(c_i)] \\ &= \frac{\delta_1 2^{c_i}}{(2^{c_i} - 1)^2} [h'_1(c_i) (2^{c_i} - 1) - \ln(2) h_1(c_i)] \\ &= \frac{-\delta_1 2^{c_i} e^{-\frac{h_0^2(c_i)}{2}} \ln(2)}{(2^{c_i} - 1)^2} \left[ \frac{\delta_1 h_0(c_i) 2^{c_i} \sqrt{2\pi}}{\ln(2)} + 1 \right]. \end{aligned} \quad (34)$$

For  $f'_{C_i}(c_i) = 0$ , some equation elements can be disregarded

$$\frac{-\delta_1 2^{c_i} e^{-\frac{h_0^2(c_i)}{2}} \ln(2)}{(2^{c_i} - 1)^2} < 0, \quad \forall c_i \in (0, \infty). \quad (35)$$

After simplifications, replacing the auxiliary terms from (30) in (34), and replacing  $c_i$  with  $\mu_{C_i}$ , results in (9).

#### APPENDIX D

##### CAPACITY CDF GIVEN THE SEMICIRCULAR $\lambda_{\text{dB}}$ DISTRIBUTION

The capacity CDF can be obtained from integrating (12). Considering  $\delta_2 = \sigma_{\text{mdg}} \ln(10) / 10$ , the CDF is given by

$$\begin{aligned} F_C(c) &= \int_{c_0}^c f_C(x) dx \\ &= \frac{\ln(2)}{2\pi\delta_2} \int_{c_0}^c \frac{2^x}{2^x - 1} \\ &\quad \sqrt{4 - \left( \frac{1}{\delta_2} \ln \left( \frac{2^x - 1}{\text{SNR}} \right) - \frac{\mu_{\lambda_{\text{dB}}}}{\sigma_{\text{mdg}}} \right)^2} dx, \end{aligned} \quad (36)$$

where  $c_0 = \log_2(\text{SNR} \cdot 10^{\frac{1}{10}(\mu_{\lambda_{\text{dB}}} - 2\sigma_{\text{mdg}})} + 1)$  is the smallest value of  $c$  such that  $f_C(c)$  is strictly real. Applying the following variable substitutions

$$\begin{aligned} y &= \sin^{-1} \left( \frac{1}{2\delta_2} \ln \left( \frac{2^x - 1}{\text{SNR}} \right) - \frac{\mu_{\lambda_{\text{dB}}}}{2\sigma_{\text{mdg}}} \right) \\ y_0 &= \sin^{-1} \left( \frac{1}{2\delta_2} \ln \left( \frac{2^{c_0} - 1}{\text{SNR}} \right) - \frac{\mu_{\lambda_{\text{dB}}}}{2\sigma_{\text{mdg}}} \right) = \frac{-\pi}{2} \\ y_f &= \sin^{-1} \left( \frac{1}{2\delta_2} \ln \left( \frac{2^c - 1}{\text{SNR}} \right) - \frac{\mu_{\lambda_{\text{dB}}}}{2\sigma_{\text{mdg}}} \right) \\ dy &= \frac{\ln(2) \cdot 2^x}{\delta_2 (2^x - 1) \sqrt{4 - 4 \cdot \sin^2(y)}} dx, \end{aligned} \quad (37)$$

results in

$$F_C(c) = \frac{2}{\pi} \int_{y_0}^{y_f} \cos^2(y) dy = \frac{1}{\pi} [\cos(y) \sin(y) + y]_{y=y_0}^{y_f}. \quad (38)$$

Applying the necessary substitutions from (37) in (38) results in the CDF given in (13).

## REFERENCES

- [1] T. Morioka, “New generation optical infrastructure technologies: “EXAT initiative” towards 2020 and beyond,” in *2009 14th OptoElectronics and Communications Conference*. IEEE, 2009, pp. 1–2.
- [2] B. J. Puttnam, G. Rademacher, and R. S. Luís, “Space-division multiplexing for optical fiber communications,” *Optica*, vol. 8, no. 9, pp. 1186–1203, 2021.
- [3] I. Cristiani, C. Lacava, G. Rademacher, B. J. Puttnam, R. S. Luís, C. Antonelli, A. Mecozzi, M. Shtaif, D. Cozzolino, D. Bacco *et al.*, “Roadmap on multimode photonics,” *Journal of Optics*, vol. 24, no. 8, p. 083001, 2022.
- [4] G. Rademacher, B. J. Puttnam, R. S. Luís, J. Sakaguchi, W. Klaus, T. A. Eriksson, Y. Awaji, T. Hayashi, T. Nagashima, T. Nakanishi *et al.*, “10.66 peta-bit/s transmission over a 38-core-three-mode fiber,” in *optical fiber communication conference*. Optica Publishing Group, 2020, pp. Th3H–1.
- [5] G. Rademacher, B. J. Puttnam, R. S. Luís, T. A. Eriksson, N. K. Fontaine, M. Mazur, H. Chen, R. Ryf, D. T. Neilson, P. Sillard *et al.*, “Peta-bit-per-second optical communications system using a standard cladding diameter 15-mode fiber,” *Nature Communications*, vol. 12, no. 1, p. 4238, 2021.
- [6] G. Rademacher, R. S. Luís, B. J. Puttnam, N. K. Fontaine, M. Mazur, H. Chen, R. Ryf, D. T. Neilson, D. Dahl, J. Carpenter *et al.*, “1.53 peta-bit/s c-band transmission in a 55-mode fiber,” in *2022 European Conference on Optical Communication (ECOC)*. IEEE, 2022, pp. 1–4.
- [7] P. J. Winzer and G. J. Foschini, “MIMO capacities and outage probabilities in spatially multiplexed optical transport systems,” *Optics express*, vol. 19, no. 17, pp. 16 680–16 696, 2011.
- [8] C. Antonelli, A. Mecozzi, M. Shtaif, and P. J. Winzer, “Modeling and performance metrics of MIMO-SDM systems with different amplification schemes in the presence of mode-dependent loss,” *Optics Express*, vol. 23, no. 3, pp. 2203–2219, 2015.
- [9] D. A. Mello, H. Srinivas, K. Choutagunta, and J. M. Kahn, “Impact of polarization-and mode-dependent gain on the capacity of ultra-long-haul systems,” *Journal of Lightwave Technology*, vol. 38, no. 2, pp. 303–318, 2020.
- [10] K.-P. Ho and J. M. Kahn, “Mode-dependent loss and gain: statistics and effect on mode-division multiplexing,” *Opt. Express*, vol. 19, no. 17, pp. 16 612–16 635, Aug 2011.
- [11] —, “Frequency diversity in mode-division multiplexing systems,” *Journal of Lightwave Technology*, vol. 29, no. 24, pp. 3719–3726, 2011.
- [12] T. W. Anderson, T. W. Anderson, T. W. Anderson, and T. W. Anderson, *An introduction to multivariate statistical analysis*. Wiley New York, 1958, vol. 2.
- [13] A. Paulraj, R. Nabar, and D. Gore, *Introduction to space-time wireless communications*. Cambridge university press, 2003.
- [14] E. P. Wigner, “Characteristic vectors of bordered matrices with infinite dimensions i,” *Annals of Mathematics*, vol. 62, no. 3, pp. 548–564, 1955.
- [15] F. J. Dyson, “A Brownian-motion model for the eigenvalues of a random matrix,” *Journal of Mathematical Physics*, vol. 3, no. 6, pp. 1191–1198, 1962.
- [16] K.-P. Ho and J. M. Kahn, “Statistics of Group Delays in Multimode Fiber With Strong Mode Coupling,” *Journal of Lightwave Technology*, vol. 29, no. 21, pp. 3119–3128, Aug 2011.
- [17] C. A. Tracy and H. Widom, “Level-spacing distributions and the Airy kernel,” *Communications in Mathematical Physics*, vol. 159, pp. 151–174, 1994.
- [18] S. Ö. Arık and J. M. Kahn, “Diversity-multiplexing tradeoff in mode-division multiplexing,” *Optics Letters*, vol. 39, no. 11, pp. 3258–3261, 2014.